NAVAL POSTGRADUATE SCHOOL
Monterey, California

THESIS

Effects of Scaling on the Performance
of Magnetoplasmadynamic Thrusters

by

Wayne M. Schmidt

June 1989

Thesis Advisor: A.E. Fuhs

SECURITY CLASSIFICATION OF THIS PAGE

REPORT DOCUMENTATION PAGE

Form Approved
OMB No. 0704-0188

1a REPORT SECURITY CLASSIFICATION Unclassified	1b RESTRICTIVE MARKINGS
2a SECURITY CLASSIFICATION AUTHORITY	3 DISTRIBUTION/AVAILABILITY OF REPORT Approved for public release; distribution is unlimited
2b DECLASSIFICATION/DOWNGRADING SCHEDULE	
4 PERFORMING ORGANIZATION REPORT NUMBER(S)	5 MONITORING ORGANIZATION REPORT NUMBER(S)
6a NAME OF PERFORMING ORGANIZATION Naval Postgraduate School 6b OFFICE SYMBOL (If applicable)	7a NAME OF MONITORING ORGANIZATION Naval Postgraduate School
6c ADDRESS (City, State, and ZIP Code) Monterey, CA 93943-5000	7b ADDRESS (City, State and ZIP Code) Monterey, CA 93943-5000
8a NAME OF FUNDING/SPONSORING ORGANIZATION 8b OFFICE SYMBOL (If applicable)	9 PROCUREMENT INSTRUMENT IDENTIFICATION NUMBER
8c ADDRESS (City, State and ZIP Code)	10 SOURCE OF FUNDING NUMBERS PROGRAM ELEMENT NO / PROJECT NO / TASK NO / WORK UNIT ACCESSION NO

11 TITLE (Include Security Classification)
Effects of Scaling on the Performance of Magnetoplasmadynamic Thrusters

12 PERSONAL AUTHOR(S)
Wayne M. Schmidt

13a TYPE OF REPORT	13b TIME COVERED	14 DATE OF REPORT (Year, Month Day)	15 PAGE COUNT
Engineer's Thesis	FROM _____ TO _____	June 1989	54

16 SUPPLEMENTARY NOTATION The views expressed in this thesis are those of the author and do not reflect the official policy or position of the Department of Defense or the U.S. Government.

17 COSATI CODES			18 SUBJECT TERMS (Continue on reverse if necessary and identify by block number)
FIELD	GROUP	SUB-GROUP	Space Electric Propulsion, plasma propulsion, scaling laws, Magnetoplasmadynamic Thrusters

19 ABSTRACT (Continue on reverse if necessary and identify by block number)

A combined theoretical and empirical numerical model was developed which predicts the performance of continuous electrode coaxial magnetoplasmadynamic thrusters as a function of thruster dimensions, mass flow rate, and input current. This model was used to predict the effects of scaling on these thrusters.

The model predicts that for scaling factors down to one-half, relations can be found relating the performance of one thruster to another. The model was used to examine these relationships for four different thruster configurations over a broad range of operating currents. The thrusters examined consisted of two geometries and their half scale counterparts. A conclusion from the analysis is that scaling down the size of the thruster by 50% can reduce the total power input by 30% to 40% at comparable efficiencie However, this is at the cost of increasing the specific impulse by a factor of two which may render the thruster inappropriate for the intended missions.

20 DISTRIBUTION/AVAILABILITY OF ABSTRACT	21 ABSTRACT SECURITY CLASSIFICATION
☒ UNCLASSIFIED/UNLIMITED ☐ SAME AS RPT ☐ DTIC USERS	Unclassified
22a NAME OF RESPONSIBLE INDIVIDUAL Professor A.E. Fuhs	22b TELEPHONE (Include Area Code) 646-2948 / 22c OFFICE SYMBOL 67Fu

DD Form 1473, JUN 86 Previous editions are obsolete SECURITY CLASSIFICATION OF THIS PAGE

S/N 0102-LF-014-6603

Approved for public release; distribution unlimited.

Effects of Scaling on the Performance of Magnetoplasmadynamic Thrusters

by

Wayne M. Schmidt
Captain, United States Air Force
B.S.M.E., California State University at Pomona, 1979
M.E. California State University at Pomona, 1979

Submitted in partial fulfillment of the
requirements for the degree of

AERONAUTICAL ENGINEER

from the

NAVAL POSTGRADUATE SCHOOL
June 1989

ABSTRACT

A combined theoretical and empirical numerical model was developed which predicts the performance of continuous electrode coaxial magnetoplasmadynamic thrusters as a function of thruster dimensions, mass flow rate, and input current. This model was used to predict the effects of scaling on these thrusters.

The model predicts that for scaling factors down to one-half, relations can be found relating the performance of one thruster to another. The model was used to examine these relationships for four different thruster configurations over a broad range of operating currents. The thrusters examined consisted of two geometries and their half scale counterparts. A conclusion from the analysis is that scaling down the size of the thruster by 50% can reduce the total power input by 30% to 40% at comparable efficiencies. However, this is at the cost of increasing the specific impulse by a factor of two which may render the thruster inappropriate for the intended missions.

TABLE OF CONTENTS

LIST OF FIGURES

LIST OF SYMBOLS

Symbols:

B - magnetic field strength (tesla)
c - specific heat (amperes/square meter)
E - electric field strength (volts/meter)
F - force (newtons)
f - force density (newtons/cubic meter)
Isp - specific impulse (seconds)
J - current (amperes)
j - current density (amperes/square meter)
M - mass (kilograms)
N - efficiency
P - pressure (newtons/square meter)
r - radial distance (meters)
T - temperature (kelvin)
t - time (seconds)
u - velocity (meters/seconds)
V - electric potential (volts)
w - propellant mass flow rate (kilograms/second)
z - thruster length (meters)
z' - axial position (meters)
Δv - velocity increment (meters/second)
μ_0 - permiability constant (henries/meter)
ρ - density (kilograms/cubic meter)
ϕ - volume specific power (watts/cubic meter)

Subscripts:

a - anode
c - cathode
e - electrothermal component or rocket engine exhaust
f - final
i - initial
l - thermal input by conduction
r - radiation or radial vector component
v - viscosity
x,y,z - cartesian coordinate components
1,2 - first and second parts of a two part equation

ACKNOWLEDGMENTS

I offer my most sincere appreciation to the management and personnel of the Air Force Astronautics Laboratory at Edwards Air Force Base. The financial, technical, and moral support they provided were invaluable to this project.

I offer my special thanks to Professor Fuhs for agreeing to take on all of the reading courses my program required and agreeing to be my thesis advisor.

Finally, I would like to acknowledge the assistance of the Naval Postgraduate School Library staff. Without their assistance in obtaining all of the reference materials required for the thesis its completion would have been impossible.

I. INTRODUCTION

Equation 1 expresses the relationship between initial and final space vehicle mass to the propellant exhaust velocity and the velocity increment required for a maneuver in space [1]. This equation shows that a rocket engine's exhaust velocity must be greater than the velocity increment of the mission of interest for a significant amount of payload to be delivered. If the exhaust velocity is much less than the velocity increment, the ratio of spacecraft masses becomes small implying a small final mass or payload. The velocity increment depends only on flight path and is independent of the vehicle. Therefore, the only way of improving the mass ratio is to increase the exhaust velocity of the rocket engine.

$$M_f/M_i = \exp(-\Delta v/u_e) \qquad (1)$$

Chemical rocket engines have a maximum exhaust velocity determined by the amount of energy stored in the chemical bonds of the fuel. This limits exhaust velocities to less than 5000 meters per second. Orbit transfer missions such as Low Earth Orbit (LEO) to Geosynchronous Orbit (GEO) require velocity increments of approximately 4200 meters per second. Application of these values to Equation 1 gives a mass ratio of less than one-half. This implies that, at best, less than half of the initial weight of a spacecraft

can be useful payload. For current space motors, the ratio of initial mass to final mass is about 4:1. An alternative to chemical propulsion is electric propulsion. Electric propulsion avoids the thermodynamic limitations of chemical engines by employing an external power source to generate the forces required to accelerate a propellant. The amount of energy available to provide thrust is no longer determined by the nature of the propellants. This enables greater amounts of energy to be applied to the propellant than possible with chemicals. One such device is the magnetoplasmadynamic (MPD) thruster. This coaxial electric propulsion device uses the Lorentz jxB force to accelerate a plasma to velocities in excess of 25,000 meters per second. This increased exhaust velocity enables a 50% to 200% increase in the mass of the delivered payload. An electrical power supply must now be included in the spacecraft mass, but the reduction in propellant mass enabled by the MPD thruster's high exhaust velocities may be suffucient to allow for the mass of the power supply. Figure 1 shows an MPD thruster.

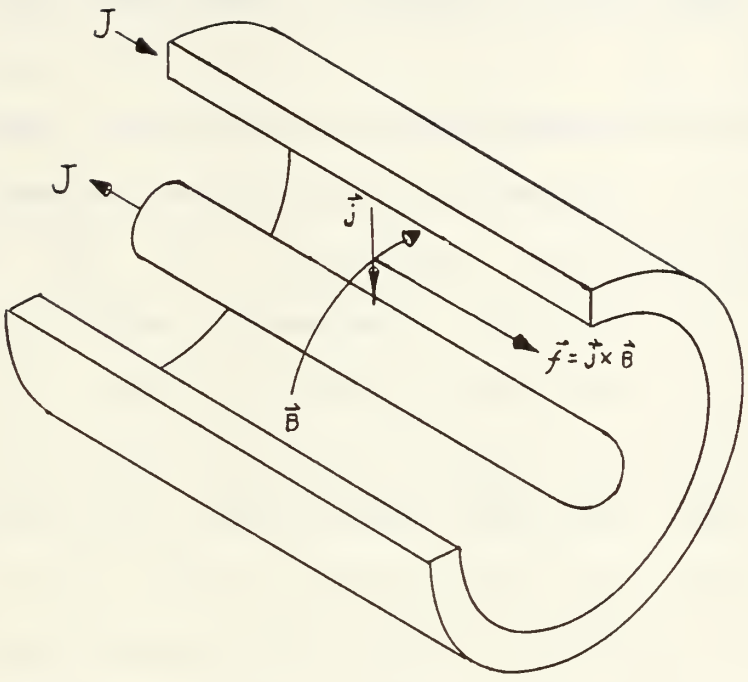

Figure 1 Continuous Electrode MPD Thruster

It can be seen that the thruster is structurally a very simple device. The MPD thruster has attracted considerable attention not only for its simplicity, but also because much greater thrust levels than any other electric propulsion device can be generated. This, combined with its ability to operate with virtually any propellant, make it a prime candidate for supporting space missions.

The price to be paid for eliminating the dependence on the chemical energy in the fuel and oxidizer is the requirement of an external power source. Power requirements for even modest sized MPD thrusters reach to the multimegawatt range.

Space based power supplies of this size will not be available for many years. Two options are available to reduce the power requirements of the thruster. The first is to increase the efficiency of the thruster design. Since these thrusters are now operating in the 50% efficiency regime [2], this technique promises a reduction in power requirements of less than a factor of two. The second option is to develop smaller thrusters which require less power than their full size counterparts. MPD thrusters, by virtue of their high thrust density, would still be able to produce useful levels of thrust after significant scaling. This technique promises much greater factors of power reduction than the first option because power requirements are related to size by a term of greater than linear scale.

It is the goal of this thesis to develop a computer model of an MPD thruster which will predict specific impulse and efficiency as functions of current, thruster dimensions, and propellant mass flow rate.

II. DERIVATION OF THE MPD THRUST MODEL

Equations 2, 3, and 4 are the equations of conservation of mass, momentum, and energy respectively.

$$\partial\rho/\partial t + \nabla\cdot(\rho\bar{u}) = 0 \tag{2}$$

$$\rho[\partial\bar{u}/\partial t + (\bar{u}\cdot\nabla)\bar{u}] = -\nabla p + (\bar{j}\times\bar{B}) + f_v \tag{3}$$

$$\rho(\partial\ /\partial t + \bar{u}\cdot\nabla)(c_pT + u^2/2) = \partial p/\partial t + \bar{j}\cdot\bar{E} + \phi_\ell + \phi_v - \phi_r \tag{4}$$

Since an MPD thruster is intended to be operated in a continuous mode, these equations can be simplified to the steady state forms of Equations 5, 6, and 7. This is justified because measurements of the start up and shut down transients in MPD thrusters are measured in seconds where as actual thruster operation is intended to last for up to 100 days [3].

$$\nabla\cdot(\rho\bar{u}) = 0 \tag{5}$$

$$\rho(\bar{u}\cdot\nabla)\bar{u} = -\nabla p + (\bar{j}\times\bar{B}) + f_v \tag{6}$$

$$\rho(\bar{u}\cdot\nabla)(c_pT + u^2/2) = \bar{j}\cdot\bar{E} + \phi_\ell + \phi_v - \phi_r \qquad (7)$$

For the derivation of an expression for the thrust of an MPD thruster Equation 6, conservation of momentum, will be of paramount importance. The low density and viscosity of the gaseous argon, which will be the propellant used, within the arc chamber suggests that the viscous drag density can be assumed negligible. Calculations [4] show that this force, when integrated over a typical thruster, is only on the order of a tenth of a Newton where as the total thrust is typically three orders of magnitude greater than this. This simplification results in Equation 8.

$$\rho(\bar{u}\cdot\nabla)\bar{u} = -\nabla p + (\bar{j}\times\bar{B}) \qquad (8)$$

It is assumed the thruster in question is a small section of an infinitely long coaxial device. This assumption greatly simplifies the mathematics by eliminating the requirement to deal with electric and magnetic field fringing and the exit plane of the thruster. In addition it will be assumed that the thruster consists of a series of coaxial streamtubes of cylindrical cross section and that

steady state migration of propellant across the stream tube boundaries does not occur. This permits the application of one dimensional analysis to the problem of modeling the forces generated by the thruster. As will be seen later, this division of the thruster into coaxial streamtubes is also necessary for the application of a numerical integration program.

The above assumptions and simplifications permit Equation 8 to be expanded using cylindrical coordinates to the form of Equation 9.

$$\rho[(\bar{u}_r+\bar{u}_\phi+u_z)\cdot(\hat{r}\partial/\partial r+\hat{\phi}\partial/\partial\phi+\hat{z}\partial/\partial z)]\cdot[\bar{u}_r+\bar{u}_\phi+\bar{u}_z] =$$
$$-[\hat{r}\partial p/\partial r+\hat{\phi}\partial p/\partial\phi+\hat{z}\partial p/\partial z]+[(\bar{j}_r+\bar{j}_\phi+\bar{j}_z)(\bar{B}_r+\bar{B}_\phi+\bar{B}_z)] \qquad (9)$$

From symmetry, the assumption that the only velocity which can be maintained is in the axial or "z" direction, and the definition of the vector dot product, Equation 9, can be simplified to Equation 10.

$$\hat{z}\rho u_z\partial u_z/\partial z = -\hat{r}\partial p/\partial r - \hat{z}\partial p/\partial z + \hat{z}j_rB_\phi - \hat{r}j_zB_\phi \qquad (10)$$

By equating vector components, Equation 10 can be split into Equations 11 and 12.

$$\rho u_z\partial u_z/\partial z = -\partial p/\partial z + j_rB_\phi \qquad (11)$$

$$0 = -\partial p/\partial r - j_zB_\phi \qquad (12)$$

After rearranging, Equation 11 can be put into the form of Equation 13 and Equation 12 becomes Equation 14.

$$f_z = u_z \partial u_z/\partial z + \partial p/\partial z = j_r B_\phi \tag{13}$$

$$f_r = -\partial p/\partial r = j_z B_\phi \tag{14}$$

It is convention [1], [5], [6]), [7], [8], [9] to refer to the f_z component as the blowing force density and the f_r component as the pumping force density. The thrust produced by an MPD thruster is, in large part, the sum of these two components integrated over the volume of the thruster. The remaining thrust is the result of electrothermal heating of the propellant as it flows through the arc chamber. Expressions for these components of thrust will be developed individually after which the three will be summed to give the total thrust.

An mathematical model for thrust can only be accomplished if the current density within the arc chamber can be mathematically defined. It has been experimentally determined [6] that over a wide range of thruster shapes and sizes, the current density follows an "S" shaped path as illustrated in Figure 2.

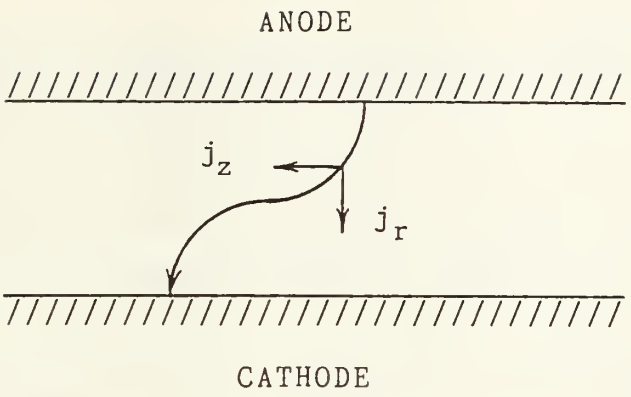

Figure 2 Current Flow Pattern Inside an MPD Thruster

For a continuous electrode thruster, the depth of this curve or amount of axial displacement is determined by the Hall parameter. For typical operating regimes, the Hall parameter varies from effectively zero to a value of approximately ten [5], [6] depending on the current for a fixed thruster. By trial and error, Equations 15 to 18 were developed and provide the current flow pattern required.

$$\text{for } r_c<r<(r_c+r_a)/2$$
$$j_r=(0.159/z\ )\{[J/r]^2-[2.22\times10^{-6}(r-r_c)J^2]^2\}^{.5} \qquad (15)$$

$$j_z = 3.54\times10^{-7}J^2(r-r_c)/z' \qquad (16)$$

For $(r_c+r_a)/2<r<r_a$

$$j_r=(0.159/z')\{[J/r]^2-[2.22\times10^{-6}(r_a-r)J^2]^2\}^{.5} \qquad (17)$$

$$j_z = 3.54\times10^{-7}J^2(r_a-r)/z \qquad (18)$$

With these relations to define the current within the thruster, expressions can be found for the blowing, pumping, and electrothermal components of thrust.

BLOWING THRUST

The blowing component of thrust results from the vector product of radial current density with an azimuthally oriented magnetic field as shown in Figure 1. Equations 15 and 17 provide the radial current densities. The magnetic field is found by applying Ampere's law for straight conductors.

$$\bar{B} = \hat{\phi}B = \hat{\phi}\mu_0 J/2\pi r \qquad \text{Ampere's Law (19a)}$$

The magnetic field which results is given in equation (19b).

$$B = (\mu_0 J/2\pi r)(1-z/z') \qquad (19b)$$

As can be seen from an examination of this equation, the magnetic field is a function both of radial and axial position within the thruster. Vector multiplication of these two crossed vectors results in a vector directed in the positive "z" direction with a magnitude defined by Equations 20 and 21.

For $r_c<r<(r_c+r_a)/2$

$$f_{z1}=(0.159J\mu_0/2\pi rz')\{[J/r]^2-[2.22\times10^{-6}(r-r_c)J^2]^2\}^{.5}(1-z/z') \qquad (20)$$

For $(r_c+r_a)/2<r<r_a$

$$f_{z2}=(0.159J\mu_0/2\pi rz')\{[J/r]^2-[2.22\times10^{-6}(r_a-r)J^2]^2\}^{.5}(1-z/z') \qquad (21)$$

These last two equations give the force density, in newtons per cubic meter, as a function of radial and axial position. To find the total blowing thrust component, it is necessary to integrate these force densities over the internal volume of the arc chamber.

For $r_c<r<(r_c+r_a)/2$

$$F_{z1} = \int_0^{z'} \int_{r_c}^{(r_c+r_a)/2} f_{z1}\,dz\,2\pi r\,dr \qquad (22)$$

For $(r_c+r_a)/2<r<r_a$

$$F_{z2} = \int_0^{z'} \int_{(r_c+r_a)/2}^{r_a} f_{z2} dz 2\pi r dr \qquad (23)$$

After integrating with respect to the axial and azimuthal variables, Equations 24 and 25 result.

$$F_{z1}=\int_{r_c}^{(r_c+r_a)/2} 7.95\times10^{4}\{[J/r]^2-[2.22\times10^{-6}(r-r_c)J^2]^2\}^{.5}Jrdr \qquad (24)$$

$$F_{z2}=\int_{(r_c+r_a)/2}^{r_a} 7.95\times10^{4}\{[J/r]^2-[2.22\times10^{-6}(r_a-r)J^2]^2\}^{.5}Jrdr \qquad (25)$$

The form of this equation is such as to resist integration analytically or through the use of generic forms given in integral tables. The total blowing force was obtained by applying numerical integration techniques to Equations 24 and 25. This integration uses the program in Appendix B titled Theoretical Model Program.

PUMPING COMPONENT

The pumping force density given by Equation 14 is the

result of the vector product of the azimuthal magnetic field and an axial component of the current in the negative "z" direction. This cross product gives rise to a force density component in the negative radial direction. This force density is balanced by a pressure gradient in the positive radial direction. Integration of the pressure gradient at the $z' = 0$ position yields an expression for pressure as a function of radial position. Multiplying pressure with a differential area and integrating provides the total pumping force.

Expanding Eequation 14 by substituting in the definitions of the axial current density and the azimuthal magnetic field at the $z' = 0$ location results in Equations 26 and 27.

For $r_c < r < (r_c + r_a)/2$

$$f_r = -\partial p/\partial r = cJ^3(r - r_c)/z'r \tag{26}$$

For $(r_c + r_a)/2 < r < r_a$

$$f_r = -\partial p/\partial r = cJ^3(r_a - r)/z'r \tag{27}$$

where $c = 7.08 \times 10^{-14}$ newtons/cm^{2}amperes^3

Separating variables and integrating gives Equations 28 and 29 which collectively represent the equation for the radial pressure gradient as a function of radial position.

For $r_c < r < (r_c + r_a)/2$

$$p = p_0 + c(r - r_c \ln r)J^3/z' \tag{28}$$

For $(r_c+r_a)/2<r<r_a$

$$p = p_0+c(r_a \ln r - r)J^3/z' \qquad (29)$$

Integrating Equations 28 and 29, with respect to a differential ring area, and collecting terms yields equation 30.

$$\begin{aligned} F_{pumping} = (2\pi cJ^3/z')\{&((r_a+r_c)2)^3/3-[((r_a+r_c)/2)^2 \cdot \\ &\ln((r_a+r_c)/2)-((r_a+r_c)/2)^2/4]-[r_c^3/3- \\ &r_c((r_c^2/2)\ln r_c-r_c^2/4)]+[(r_a^3/2)\ln r_a- \\ &r_a^3/4-r_a^3/3]-[r_a(((r_a+r_c)/2)^2/2)\ln((r_a \\ &+r_c)/2)-r_a((r_a+r_c)/2)^2/4-((r_a+r_c)/2)^3/3]\} \end{aligned} \qquad (30)$$

While this expression is long, it is algebraically simple and is easily evaluated numerically. Like the blowing thrust term, Equation 30 has been included in the Appendix B program.

ELECTROTHERMAL THRUST

Due to ohmic heating the propellant in an MPD arc chamber increases in temperature from an initial 288 K to

temperatures exceeding 20,000 K at some locations within the thruster. Cory [4] derived an expression for the electrothermal thrust based on the assumptions of negligible viscous forces, uniform pressure on the chamber walls, and no thruster pressure present on the outside surfaces of the arc chamber. His result for the pressure is presented here as Equation 31.

$$p = 3.02\times10^{-3} J^{1.5} \dot{m}^{.3} \tag{31}$$

Multiplying this expression by the exit plane area of the thruster provides an expression for the electrothermal component of thrust. This expression is Equation 32.

$$F_e = 3.02\times10^{3} J^{1.5} m^{3} [\pi(r_a^2 - r_c^2)] \tag{32}$$

TOTAL THRUST

As stated before, the total thrust is the sum of the three thrust components. A Fortran program titled Theoretical Model Program given in Appendix B performs the summation. The results of calculations using this model are discussed in section III.

THRUSTER VOLTAGE

An emperical expression for thruster voltage was assembled using all available information on coaxial MPD thrusters tested to date, [2], (3), [4], [5],[6], [8], (10), and [11]. First, an equation for voltage as a function of thruster length was developed. Second, the influence of thruster diameter was included. Finally, the influence of mass flow rate was incorporated into the equation. This voltage model was tested using thruster geometries not used in its formulation. The model predicted interpolated voltages to within three percent and extrapolated voltages within seven percent. Both of these errors are within the plus-or-minus 10 to 30 percent error bars typical of laboratory testing associated with MPD thruster operation. Therefore, the voltage model was judged to be acceptable. This model is represented by Equation 33.

$$V=((55.4-26.31*(1-r_a/5.1)-23.4*(1-Z/21.6))-((39.2-65.8*(1-r_a/5.1)-27.7*(1-Z/21.6))*1E-4*J+((35.7-54.5*(1-r_a/5.1)+3.88*(1-Z/21.6))*1E-8)*J^2)*(178.0-47.3*1000.0*W+4.3*(1000.0*W)^2)/49.0 \quad (33)$$

In this equation, z represents the thruster length and W the propellant mass flow rate.

SUMMARY

From the input parameters of thruster length (z), anode radius (r_a), cathode radius (r_c), current (J), and mass flow rate (W), the model predicts thrust and voltage. These predictions are used in Equations 34 and 35 to calculate specific impulse (Isp) and efficiency (N) respectively.

$$Isp = T/(W*9.8) \tag{34}$$

$$N = (0.5*W*(ISP*9.8)^2/(V*J) \tag{35}$$

The model has been written as a Fortran program titled Theoretical Model Program. A copy is included in this thesis as Appendix B.

III. APPLICATION AND RESULTS OF THE THEORETICAL MODEL

The theoretical computer model was tested over a wide range of input currents of known thrusters. Graphs of efficiency versus specific impulse matched the experimental results [6] to within plus or minus ten percent. Similar agreement was obtained for graphs of efficiency versus input power. The plus or minus ten percent criteria was deemed acceptable because it placed the model's plots within the error bar of the experimental data. This test verified the model's accuracy.

The model was used to predict the specific impulse and efficiency of four different thrusters over a range of current levels. The thrusters were chosen with geometries which grouped them into two pairs of full and half sized devices. All thrusters were assumed to be using argon as propellant. A coded designator was created for each device to make identification easier. This designator is of the form A/B/C/D. A is the thruster length. B is the anode radius. C is the cathode diameter. D is the mass flow rate of the argon propellant in kilograms per second. All dimensions are in centimeters. Thus a 20/5/1/.006 thruster is 20 centimeters long with a 5 centimeter inside anode radius and a 1 centimeter diameter cathode. The mass flow rate is 6 grams per second. Thruster sizes, aspect ratios,

mass flow rates, and applied currents are all consistent with those regimes of operation typical of MPD devices. Very small devices operating at power levels or mass flow rates where previous theoretical or experimental evidence indicated operation would be unstable were not examined.

The four thrusters examined were 20/5/1/.006, 10/5/1/.006 and their half scale analogs 10/2.5/.5/.0015, 5/2.5/.5/.0015 respectively. The 10/5/1/.006 configuration was chosen because it closely models the Princeton Benchmark thruster for which significant theoretical and experimental results exist. The 20/5/1/.006 thruster was selected because recent research indicates thrusters with extended electrodes are more efficient than shorter electrode thrusters like the Benchmark. The mass flow rate for the half scale thrusters was reduced by the square of the scale factor to reflect the reduction in exhaust area. This maintains a constant atomic particle density. Failure to do so would place the scaled thrusters in a completely different operating regime. Parameters for each of these devices became the input to the computer model with a range of currents from 1,000 to 25,000 amperes. The model's outputs were plotted and are presented in Figures 3 through 7 inclusive.

Figures 3 through 5 show the relationship between specific impulse and efficiency. A comparison between the

graphs for 10/5/1/.006 and 20/5/1/.006, Figure 3, discloses that, as predicted, the longer configuration is more efficient at a given specific impulse. The same result is observed in Figure 4 for the half scale thrusters. This can be explained by examining the change in current density and current patterns as thruster lengths increase. For a given current, a longer device has a lower average current density. This results in lower collision frequencies and, therefore, smaller Hall currents. Hall currents, in MPD thrusters, travel in the axial direction and are the result of the combined effects of differing collision rates and mobilities between electrons and ions. It is the Hall current which creates the pumping component of thrust. Equation 18 is an emperically derived expression for the Hall current. Because this component involves propellant being accelerated through radia pressure gradients and a 90 degree turn to exit the thruster, it is less efficient than the blowing component which is axially oriented throughout the acceleration process. This result could have been predicted by examining the relative magnitudes of the forces from Equations 24, 25, and 29. Qualitatively, both the blowing and pumping thrust components are functions of total current raised to the third power. However, the multiplicative constant for the blowing force appears to be larger than any value expected from the corresponding constant in the pumping equation. One would expect this phenomena to continue until viscous losses increase up to

large enough values to offset any gains realized by further increases in thruster length. These viscous loss effects were introduced to the model through the use of emperical data used in the formulation of the expression for thruster voltage. The dominance of the blowing component of thrust can also be observed by comparing the curves for thrusters 10/5/1/.006 and 10/2.5/.5/.0015 in Figure 5. These thrusters are the same length but the 10/2.5/.5/.0015 thruster one half the radius of the 10/5/1/.006 thruster. This results, again, in an increased average current density and the corresponding decrease in efficiency for the smaller diameter thruster for constant specific impulse.

Comparing the full size thrusters to their scaled counterparts discloses the scaled thrusters appear more efficient at a given specific impulse. This would seem to contradict the explanation of current density losses in the previous paragraphs. However, examination of Figures 6 and 7 show that the efficiencies of subscale thrusters are quadratic in nature as opposed to more linear in the full size thrusters when plotted against power. A continuation of the plots for the scaled thrusters to higher powers results in crossing of the full size and subscale thruster plots making subscale thrusters less efficient than the full sized thrusters. This behavior is indicative of the presence of a higher order loss mechanism beginning to dominate thruster operation at high specific power levels. This higher order term is most likely a reflection of frozen

flow losses being introduced with the empirical elements used in the formulation of the computer model. Frozen flow losses are the result of energy stored in the excited states of the propellant as it is exhausted. As the propellant is heated and ionized, energy is stored it the excited states. The propellant is exhausted while in an excited state resulting in an energy loss. The density of MPD thruster exhausts are too low to have collision rates high enough to de-energize these excited states and recoupe this energy in nozzles of any practical length. Frozen flow losses are related to the energy density of the propellant. Smaller thrusters operating at approximately the same power have greater amounts of energy per unit propellant mass and unit time because they have less mass in which to deposit the energy. This effect is present throughout the range of operating conditions but is more pronounced at high power due to the increased occurrence of secondary ionizations.

Figures 6 and 7 are plots of efficiency versus input power for the four thrusters examined. These graphs show that scaled thrusters can be expected to operate at lower power levels than their full sized counterparts along lines of constant efficiency. This phenomena, as the above explanation presents, is restricted to the lower power regimes of operation. The graphs show that overall power requirements can be reduced by using subscale thrusters. What is also shown is that for scaled thrusters operating along lines of constant efficiency, the smaller thrusters

have much higher specific impulses. This is not necessarily an additional benefit. Operationally, a propulsion system has a minimum total mass for a given total impulse requirement determined in part by the specific impulse [1]. Operating at specific impulses above the optimum point can result in an increase in propulsion system mass. This is the consequence of power supply mass exceeding the optimum value. The graphs show a one half reduction in linear scale results in a 30% to 40% reduction in power requirements for thruster operation in the 10% to 20% efficiency regime. This is accompanied by a 40% to 60% increase in specific impulse over the same range of efficiencies.

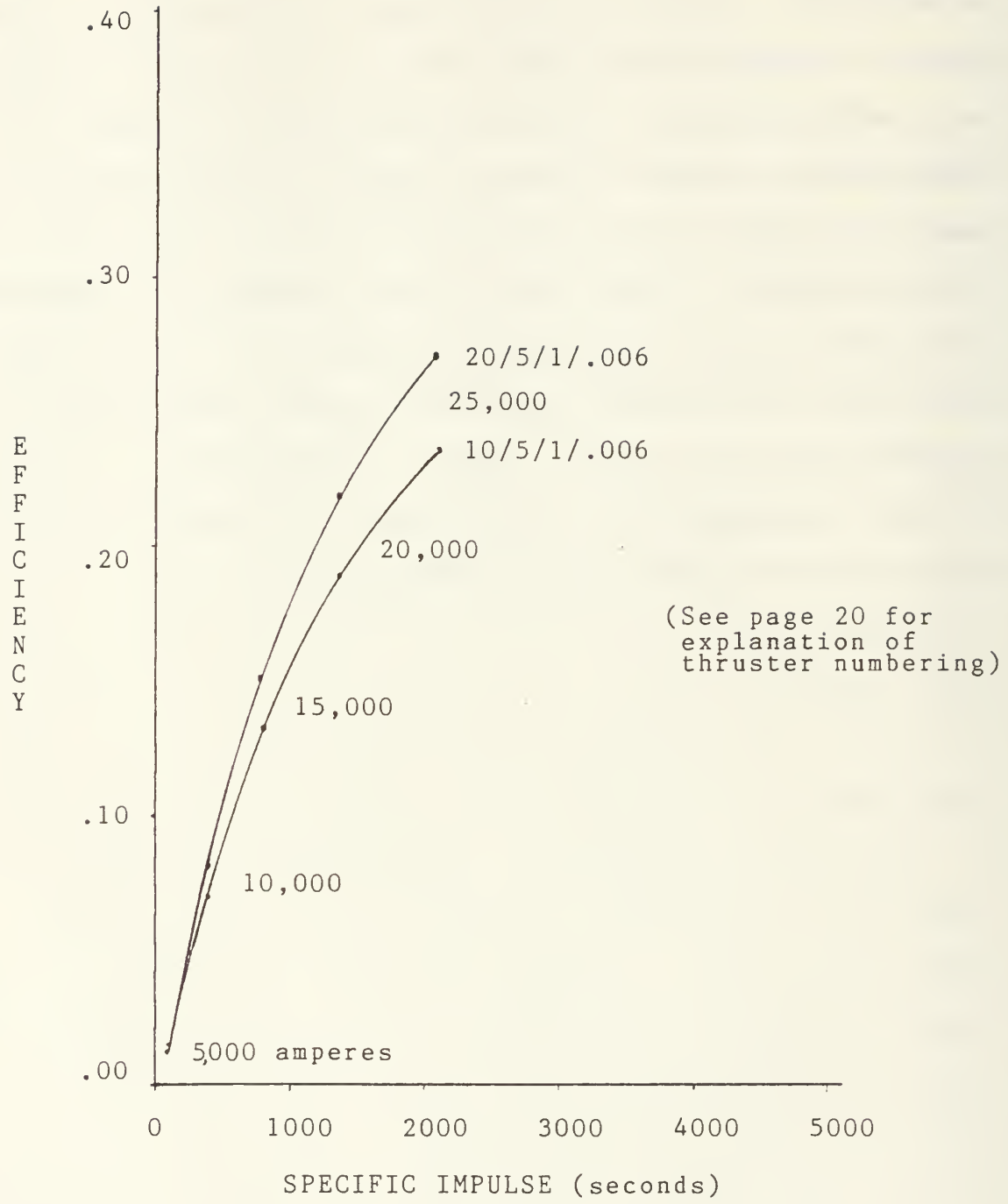

Efficiency versus Specific Impulse for 20/5/1/.006 and 10/5/1/.006 MPD Thrusters

FIGURE 3

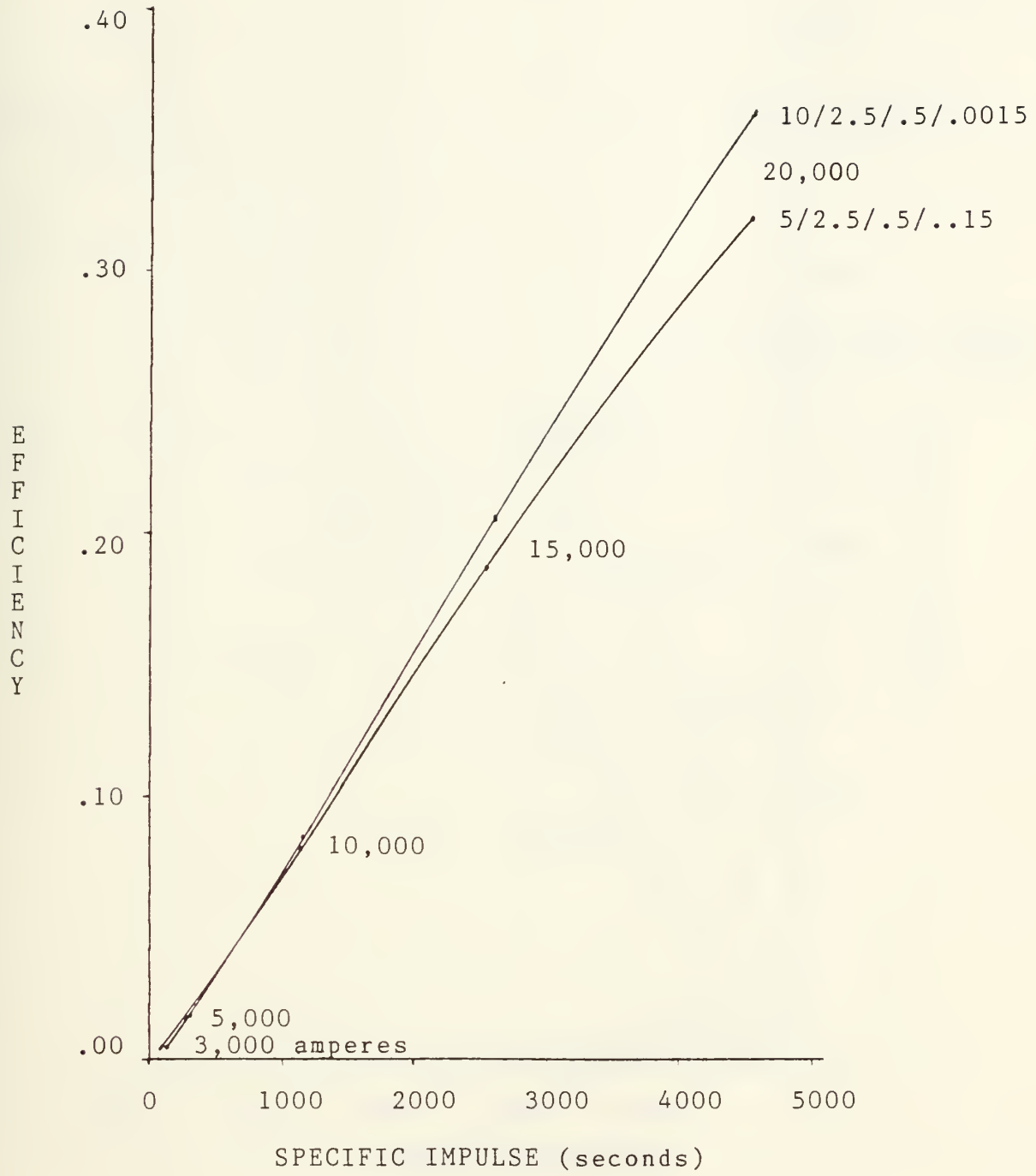

Efficiency versus Specific Impulse for 10/2.5/.5/0015 and 5/2.5/.5/.0015 MPD Thrusters

FIGURE 4

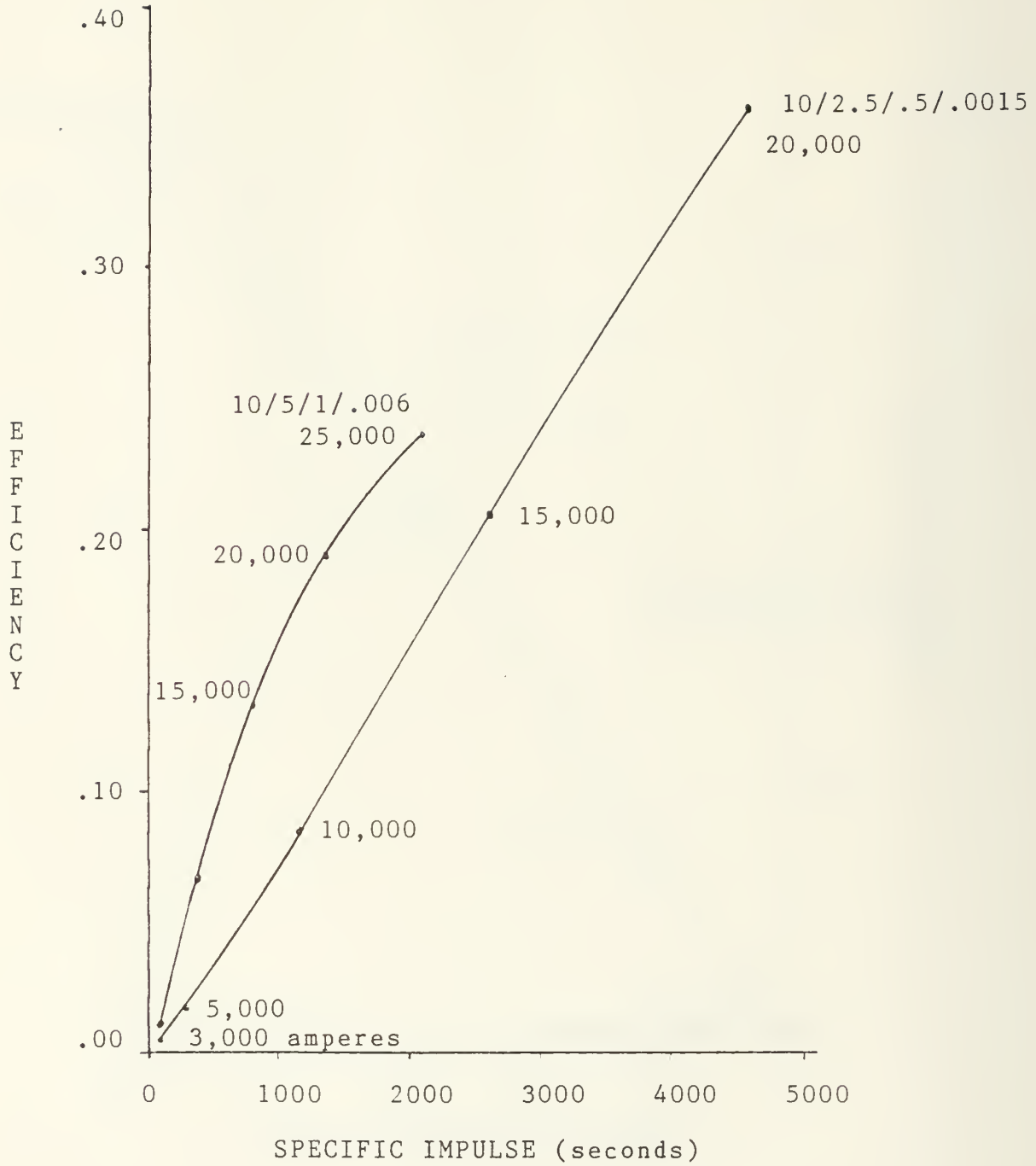

Efficiency versus Specific Impulse for 10/2.5/.5/.0015 and 10/5/1/.006 MPD Thrusters

FIGURE 5

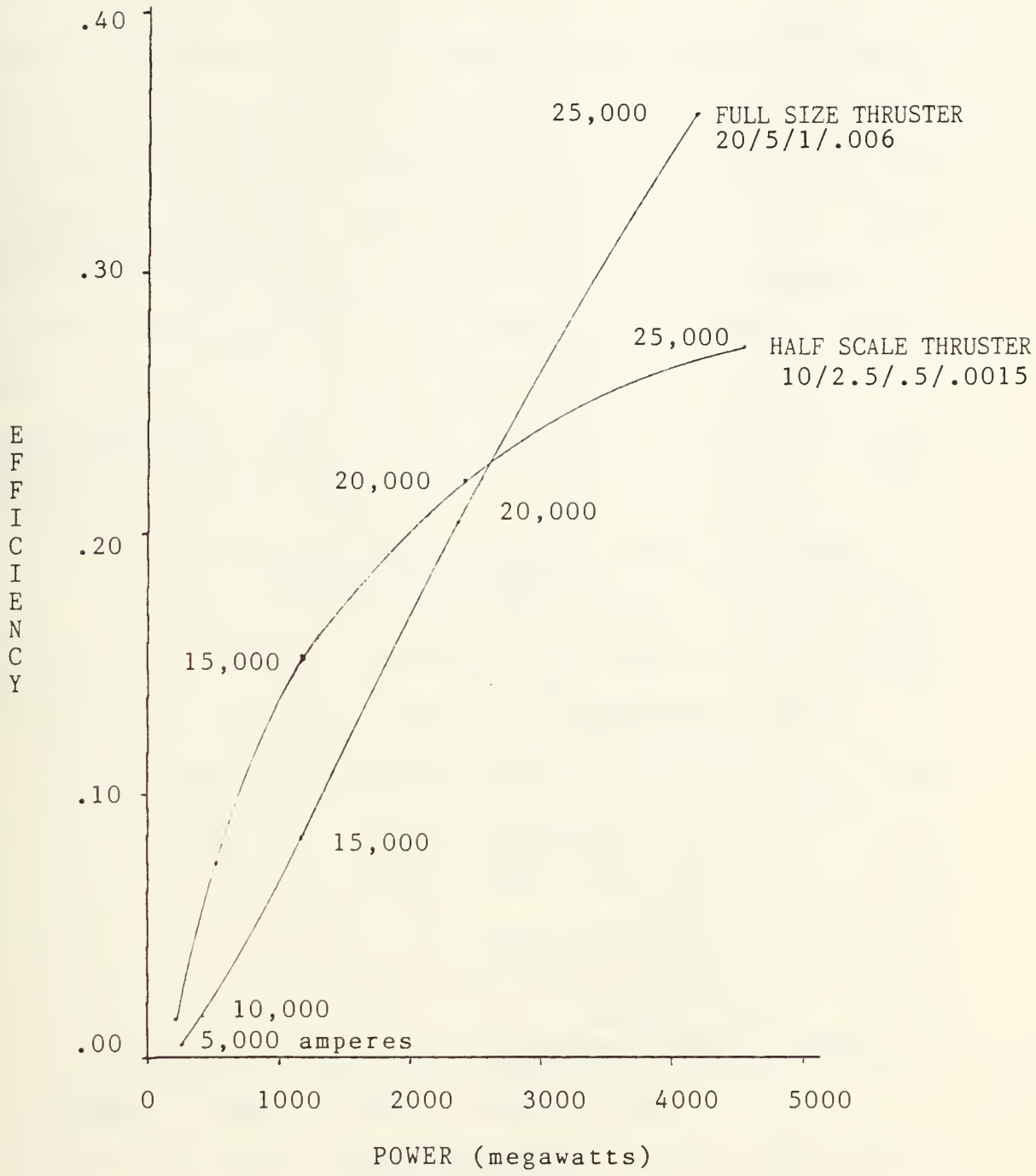

Theoretical Graph of Efficiency versus Input Power for Full Size and 1/2 scale MPD Thrusters Based on the 20/5/1/.006 MPD Thruster

FIGURE 6

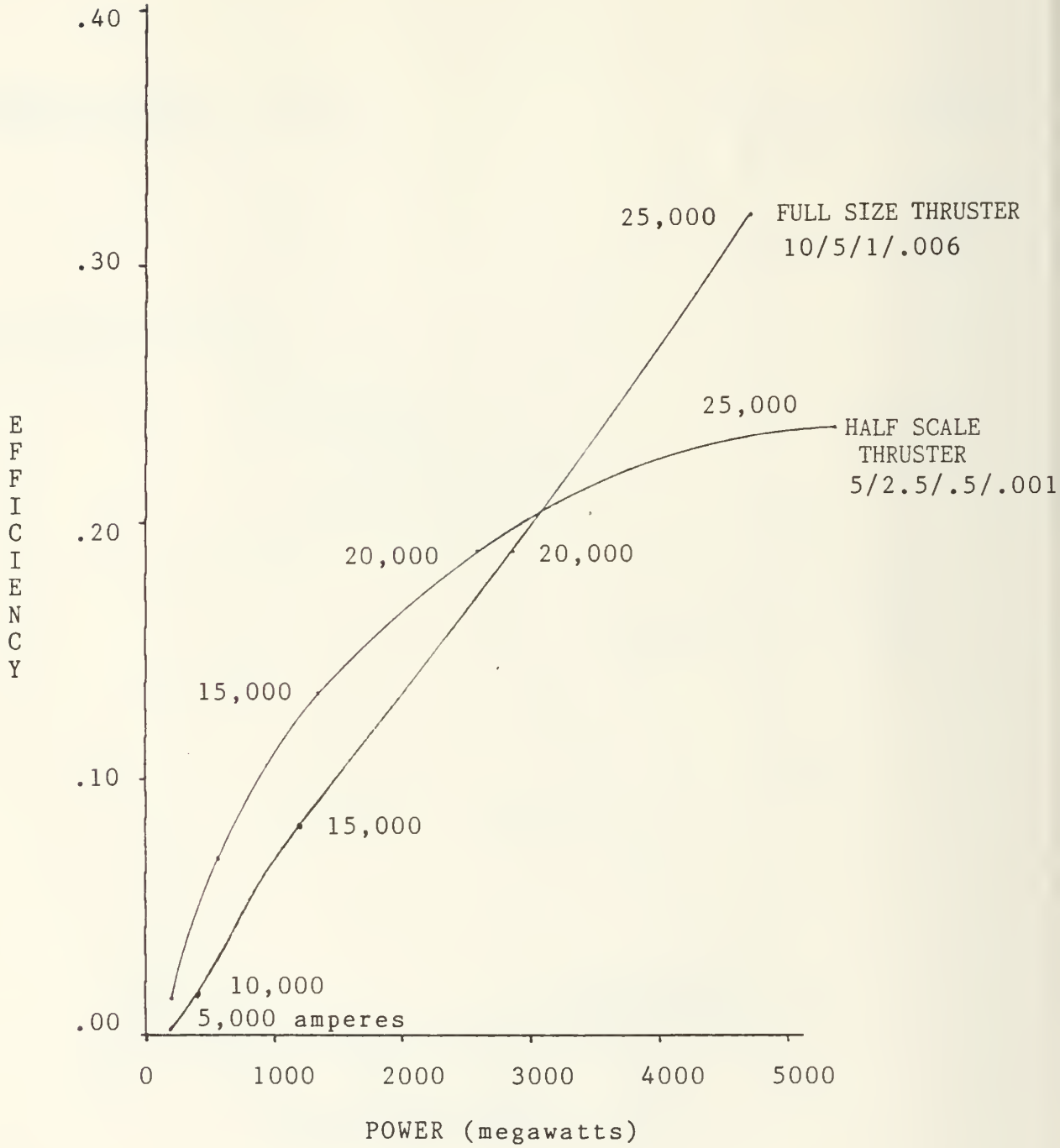

Theoretical Graph of Efficiency versus Input Power for Full Size and 1/2 scale MPD Thrusters Based on the 10/5/1/.00600 MPD Thruster

FIGURE 7

IV. CONCLUSIONS AND RECOMMENDATIONS FOR FUTURE RESEARCH

The data generated by the computer model indicates scaled thrusters can operate at comparable efficiencies to full size thrusters but at reduced power levels. The reduction in power is on the order of 30% to 40% for linear geometrical scale factors of one half. While this reduces the power requirements for an operational system thereby making it more plausible, this reduction in power is accompanied by an even greater increase in specific impulse. The increase in specific impulse is on the order of 40% to 60% putting the subscale MPD thruster into the 2500 sec regime. Studies [8] indicate orbit transfer missions are optimized with specific impulses in the 1600 second to 2000 second regime. Scaling of MPD thrusters may result in operation at specific impulses higher than optimum, thereby reducing the amount of payload such a propulsion system could deliver. This, coupled with the fact that this phenomena only occurs in the undesirably low efficiency range of 10% to 20%, indicates scaling thrusters to reduce power requirements may not be a good choice when developing an operational system.

Much work remains to be completed to verify this model. This will require extensive testing of a wide variety of different MPD thrusters and their scaled counterparts. An

attempt to do this is now underway in the Air Force Astronautics Laboratory's Electric Propulsion Laboratory. However, approximately two years of work remain before sufficient empirical data is generated to verify and further refine and expand the model. Once that is done, the model will be a valuable tool for the prediction of thruster performance. Appendix A is a data reduction program written in Fortan and intended for use in this Laboratory once the test apparatus is functional. An example of its output follows the program.

```
      PROGRAM MPD
      CHARACTER HH*9,II*4
      REAL V(40),U(40),W(40),VA(20),UA(20),WA(20),SI(40),SIA
     1(20),F(40),FA(20),E(40),EA(20)
      WRITE(*,106)
106   FORMAT(1x,'THIS PROGRAM ACCEPTS UP TO 33 DATA POINTS')
984   CONTINUE
      WRITE(*,101)
101   FORMAT(1X,'ENTER THE CATHODE LENGTH, ANODE LENGTH, '
     1,'(IN CM), AND SCALE FACTOR IN F4.1')
      READ(*,102) XX,YY,ZZ
102   FORMAT(3F4.1)
      WRITE(*,001)
001   FORMAT(1X,'ENTER THE DATE AND TIME ACCORDING TO '
     1,'AIR FORCE CONVENTION')
      READ(*,002) HH,II
002   FORMAT(A9,A4)
      WRITE(*,981)
981   FORMAT(1X,'ENTER THE MASS FLOW RATE IN KG/S IN F6.4')
      READ(*,086) DM
086   FORMAT(F6.4)
      DMM=DM*1000.
      WRITE(*,199)
199   FORMAT(1X,'HIT CONTROL-P THEN RETURN TO PRINT INTRO.'
     1,'AFTER PRINTING, REPEAT THE COMMANDS AND REWIND THE'
     2,' PAPER TO THE TOP.')
      READ(*,198) KP
198   FORMAT(A1)
      WRITE(*,200)
200   FORMAT(9X,' _____ ')
      WRITE(*,201)
201   FORMAT(9X,'|  THIS  DATA  WAS OBTAINED FROM |')
      WRITE(*,202)
202   FORMAT(9X,'| THE   VARIABLE   GEOMETRY  MPD |')
      WRITE(*,203)
203   FORMAT(9X,'| THRUSTER   AT  THE  AIR  FORCE |')
      WRITE(*,204)
204   FORMAT(9X,'| ROCKET  PROPULSION  LABORATORY |')
      WRITE(*,003) HH,II
003   FORMAT(9X,'| ON  ',A9,'  AT  ',A4,' HOURS. |')
      WRITE(*,205)
205   FORMAT(9X,'| VOLTAGE (V)   AND  CURRENT (J) |')
      WRITE(*,206)
206   FORMAT(9X,'| MEASUREMENTS WERE READ FROM AN |')
      WRITE(*,207)
207   FORMAT(9X,'| OSCILLOSCOPE  ATTACHED  TO THE |')
      WRITE(*,208)
208   FORMAT(9X,'| THRUSTER ELECTRODES. THE TOTAL |')
      WRITE(*,209)
```

```
209 FORMAT(9X,'| IMPULSE (TI)  WAS TAKEN FROM A |')
    WRITE(*,210)
210 FORMAT(9X,'| TIME INTEGRATED ACCELEROMETER. |')
    WRITE(*,211)
211 FORMAT(9X,'| TOTAL GAS PULSE  IMPULSE (TIG) |')
    WRITE(*,212)
212 FORMAT(9X,'| WAS  OBTAINED  FROM FIRING THE |')
    WRITE(*,213)
213 FORMAT(9X,'| THRUSTER  WITH  THE ELECTRODES |')
    WRITE(*,214)
214 FORMAT(9X,'| SHORTED.   THE DURATION OF THE |')
    WRITE(*,215)
215 FORMAT(9X,'| THRUST  PULSE (DT)  CAME  FROM |')
    WRITE(*,216)
216 FORMAT(9X,'| MEASURING THE TIME BETWEEN THE |')
    WRITE(*,217)
217 FORMAT(9X,'| HALF CURRENT POINTS  ON A PLOT |')
    WRITE(*,218)
218 FORMAT(9X,'| OF CURRENT VS TIME.  THE  RISE |')
    WRITE(*,219)
219 FORMAT(9X,'| AND  FALL  OF THE CURRENT  WAS |')
    WRITE(*,220)
220 FORMAT(9X,'| FAST  ENOUGH  TO  JUSTIFY  THE |')
    WRITE(*,221)
221 FORMAT(9X,'| SQUARE PULSE SHAPE  ASSUMPTION |')
    WRITE(*,222)
222 FORMAT(9X,'| INHERENT  IN  THIS  PROCEDURE. |')
    WRITE(*,223)
223 FORMAT(9X,'| THE  MASS  FLOW  RATE(DM)  WAS |')
    WRITE(*,224)
224 FORMAT(9X,'| DETERMINED  BY  MEARURING  THE |')
    WRITE(*,225)
225 FORMAT(9X,'| SHAPE  OF  THE GAS PULSE  WITH |')
    WRITE(*,226)
226 FORMAT(9X,'| AN  ION  GAUGE  AND  COMBINING |')
    WRITE(*,227)
227 FORMAT(9X,'| THIS WITH  THE MASS LOST  FROM |')
    WRITE(*,228)
228 FORMAT(9X,'| A PLENUM TO THE GAS VALVE.     |')
    WRITE(*,229)
229 FORMAT(9X,'|  CALCULATED DATA  WAS OBTAINED |')
    WRITE(*,230)
230 FORMAT(9X,'| FROM  THE MEASURED DATA  USING |')
    WRITE(*,231)
231 FORMAT(9X,'| THE FOLLOWING EQUATIONS:       |')
    WRITE(*,400)
400 FORMAT(9X,'|    THRUST(T) = (TI-TIG)/DT     |')
    WRITE(*,234)
234 FORMAT(9X,'| SPECIFIC IMPULSE = T/(9.8*DM)  |')
    WRITE(*,236)
```

```
236 FORMAT(9X,'|  EFFICIENCY = T**2/(2*V*J*DM)  |')
    WRITE(*,238)
238 FORMAT(9X,'|  AVERAGES  OF REPEATED FIRINGS |')
    WRITE(*,239)
239 FORMAT(9X,'| ARE SENT TO A PLOTTING PROGRAM |')
    WRITE(*,240)
240 FORMAT(9X,'| WHICH FITS  A SPLINED CURVE TO |')
    WRITE(*,241) XX,YY,ZZ,DMM
241 FORMAT(9X,'| THEM. THRUSTER #',3F4.1,F2.0,' |')
    WRITE(*,242)
242 FORMAT('+                 ____________________________________'
   1,'_')
    READ(*,243) IK
243 FORMAT(A1)
836 CONTINUE
    I=1
    L=0
009 CONTINUE
    WRITE(*,010) I
010 FORMAT(1X,'ENTER VOLTAGE DATA POINT NUMBER ',I2)
    READ(*,011) V(I)
011 FORMAT(F5.1)
    WRITE(*,012) I
012 FORMAT(1X,'ENTER CURRENT DATA POINT NUMBER ',I2)
    READ(*,013) U(I)
013 FORMAT(F6.0)
    WRITE(*,014) I
014 FORMAT(1X,'ENTER TOTAL IMPULSE DATA POINT NUMBER ',I2)
    READ(*,015) W(I)
015 FORMAT(F5.3)
    WRITE(*,950)
950 FORMAT(1X,'TO CORRECT ANY OF THE LAST THREE VALUES, '
   1,'ENTER A 1 AND ENTER THE NEW NUMBERS.   OTHERWISE '
   2,'ENTER A 0.')
    READ(*,951) JM
951 FORMAT(I1)
    IF(JM.EQ.1) GO TO 009
    WRITE(*,016)
016 FORMAT(1X,'IF THIS IS THE LAST OR ONLY ELEMENT OF A '
   1,'GROUPING OF DATA POINTS TO BE AVERAGED TO MAKE '
   2,'A SINGLE POINT FOR PLOTTING, ENTER THE NUMBER OF'
   3,' ELEMENTS IN THE GROUP. IF IT IS NOT THE LAST'
   4,' ELEMENT IN A GROUP ENTER A 0.')
    READ(*,017) NN
017 FORMAT(I1)
    IF(NN.EQ.0) GO TO 20
    L=L+1
    VA(L)=0.0
    UA(L)=0.0
    WA(L)=0.0
```

```
      M=I+1-NN
      DO 018 J=M,I
      VA(L)=VA(L)+V(J)
      UA(L)=UA(L)+U(J)
      WA(L)=WA(L)+W(J)
018   CONTINUE
      VA(L)=VA(L)/NN
      UA(L)=UA(L)/NN
      WA(L)=WA(L)/NN
      WRITE(*,600)
600   FORMAT(1X,'THE AVERAGES FOR THIS GROUP ARE')
      WRITE(*,450) VA(L),UA(L),WA(L)
450   FORMAT(1X,F10.5,'VOLTS',F10.2,'AMPS',F10.5,'NEWTON-S'
     1,'ECONDS')
020   CONTINUE
      WRITE(*,30)
030   FORMAT(1X,'ENTER A 1 IF YOU HAVE MORE DATA POINTS.'
     1,'ENTER A ZERO IF YOU ARE DONE.')
      READ(*,040) K
040   FORMAT(I1)
      IF(K.EQ.0) GO TO 045
      I=I+1
      GO TO 009
045   CONTINUE
      MM=I
      WRITE(*,046) MM,L
046   FORMAT(1X,'YOU HAVE ENTERED ',I2,' DATA POINTS'
     1,' CONSISTING OF ',I2,' GROUPS.')
831   CONTINUE
      WRITE(*,050)
050   FORMAT(1X,'ENTER THE TOTAL IMPULSE FOR THE GAS PULSE')
      READ(*,060) TIG
060   FORMAT(F5.4)
      WRITE(*,070)
070   FORMAT(1X,'ENTER THE TIME BETWEEN THE ONE-HALF '
     1,'CURRENT POINTS FOR  A TYPICAL FIRING  OF '
     2,'THETHRUSTER')
      READ(*,080) DT
080   FORMAT(F6.4)
      WRITE(*,085)
085   FORMAT(1X,'ENTER A CONTROL-P, THEN ENTER A BLANK TO'
     1,' PRINT THE DATA. AFTER THE DATA IS PRINTED, DO THE'
     2,' SAME THING TO TURN THE PRINTER OFF.')
      READ(*,089) NP
089   FORMAT(A1)
      WRITE(*,103)
103   FORMAT(46X,'_____________________________________________'
     1,'_____________')
      WRITE(*,104) XX,YY,ZZ
```

```
104 FORMAT(45X,'|CATHODE=',F4.1,' CM |ANODE='
   1, F4.1,' CM|BENCHMARK SCALE=',F4.1,'|')
    WRITE(*,105)
105 FORMAT('+                                                '
   1,'     ____________________________________________________'
   2,'__________')
    WRITE(*,350)
350 FORMAT(46X,'____________________________________________________'
   1,'______________')
    WRITE(*,351)
351 FORMAT(45X,'| GAS IMPULSE |THRUST PULSE DURATION'
   1,'|MASS FLOW RATE |')
    WRITE(*,352)
352 FORMAT('+                                                '
   1,'     ____________________________________________________'
   2,'__________')
    WRITE(*,353) TIG,DT,DM
353 FORMAT(45X,'|',1X,F5.4,'(N-S)',2X,'|',6X,F6.4,
   1,'(S)',6X,'|',1X,F6.4,'(KG/S)',2X,'|')
    WRITE(*,354)
354 FORMAT('+                                                '
   1,'     ____________________________________________________'
   2,'__________')
    WRITE(*,300)
300 FORMAT(46X,'____________________________________________________'
   1,'______________')
    WRITE(*,087)
087 FORMAT(45X '|VOLTAGE|AMPERES|TOTAL IMP.(N-S)|'
   1,' ISP |EFFICIENCY(%)|')
    WRITE(*,500)
500 FORMAT('+                                                '
   1,'     ____________________________________________________'
   2,'________')
    DO 090 I=1,MM
    F(I)=(W(I)-TIG)/DT
    E(I)=100.0*F(I)**2.0/(V(I)*U(I)*DM*2.0)
    SI(I)=F(I)/(DM*9.8)
    WRITE(*,088) V(I),U(I),W(I),SI(I),E(I)
088 FORMAT(45X,'|  ',F5.1,1X,'|',1X,F6.0,'|',4X,F5.3,6X,
   1,'|',F5.0,'|',5X,F4.1,4X,'|')
090 CONTINUE
    WRITE(*,301)
301 FORMAT('+                                                '
   1,'     ____________________________________________________'
   2,'________')
    READ(*,093) NA
093 FORMAT(A1)
    DO 100 IN=1,L
    FA(IN)=(WA(IN)-TIG)/DT
    EA(IN)=100.0*FA(IN)**2.0/(VA(IN)*UA(IN)*DM*2.0)
```

```
      SIA(IN)=FA(IN)/(DM*9.8)
  100 CONTINUE
      WRITE(*,120)
  120 FORMAT(1X,'THE AVERAGE GROUP VALUES ARE.')
      DO 150 I=1,L
      WRITE(*,130) VA(I),UA(I),WA(I),FA(I),SIA(I),EA(I)
  130 FORMAT(1X,F5.1,1X,'|',1X,F6.0,'|',5X,F5.3,8X,'|',2X
     1,F5.1,2X,'|',F5.0,'|',4X,F4.1)
  150 CONTINUE
      READ(*,700) NB
  700 FORMAT(A1)
      DO 979 III=1,L
      UA(III)=UA(III)/1000.
  979 CONTINUE
      WRITE(*,832)
  832 FORMAT(1X,'ENTER A 1 IF YOU NEED TO ENTER A NEW')
      WRITE(*,833)
  833 FORMAT(1X,'TIME OR MASS FLOW RATE              ')
      WRITE(*,834)
  834 FORMAT(1X,'ENTER A 2 TO START OVER, A 3 TO GO ON')
      READ(*,835) NNN
  835 FORMAT(I1)
      IF(NNN.EQ.1) GO TO 831
      IF(NNN.EQ.2) GO TO 836
  980 CONTINUE
      WRITE(*,841)
  841 FORMAT(1X,'ENTER 990099 FOR CRT DISPLAY')
      WRITE(*,842)
  842 FORMAT(1X,'ENTER 965030 FOR A COM2 PLOTTER')
      WRITE(*,985)
  985 FORMAT(1X,'ENTER 960030 FOR A COM1 PLOTTER')
      READ(*,843) IO,MO
  843 FORMAT(I4,I2)
      IF(IO.EQ.9900) IO=IO/100
      WRITE(*,972)
  972 FORMAT(1X,'ENTER THE LINE SEGMENT LENGTH')
      READ(*,973) Z
  973 FORMAT(F6.4)
      VA(L+1)=0.0
      VA(L+2)=60.0
      UA(L+1)=0.0
      UA(L+2)=6.0
      EA(L+1)=0.0
      EA(L+2)=10.0
      SIA(L+1)=0.0
      SIA(L+2)=1000.0
      CALL PLOTS(0,IO,MO)
      CALL WINDOW(0.,0.,10.7,7.5)
      CALL PLOT(2.6,1.3,-3)
```

```
      CALL SYMBOL(-.4,4.3,.16,CHAR(0),90.0,-1)
      CALL SYMBOL(-1.15,4.2,.16,CHAR(2),90.0,-1)
      CALL SYMBOL(-1.9,5.1,.16,CHAR(1),90.0,-1)
      CALL SYMBOL(-1.85,4.5,.16,' = ',90.0,3)
      CALL LINE(UA,VA,L,1,-1,0)
      CALL CURVE(UA,VA,L,Z)
      CALL LINE(UA,EA,L,1,-1,2)
      CALL CURVE(UA,EA,L,Z)
      CALL LINE(UA,SIA,L,1,-1,1)
      CALL CURVE(UA,SIA,L,Z)
      CALL STAXIS(.1,.16,.1,.05,-1)
      CALL AXIS(0.,0.,'CURRENT(KA)',-13,7.0,0.0,UA(L+1),U
     1A(L+2))
      CALL AXIS(0.,0.,'VOLTAGE(VOLTS) = ',17,6.0,90.0,VA(
     1L+1),VA(L+2))
      CALL AXIS(-.75,0.,'EFFICIENCY(%) = ',16,6.0,90.0,EA
     1(L+1),EA(L+2))
      CALL AXIS(-1.5,0.,'SPECIFIC IMPULSE',16,6.0,90.0,SIA(
     1L+1),SIA(L+2))
      SIA(L+2)=500.
      SI(MM+1)=0.0
      SI(MM+2)=500.
      E(MM+1)=0.0
      E(MM+2)=10.0
      CALL PLOT(0.0,0.0,-999)
      CALL WINDOW(0.,0.,10.7,7.5)
      CALL PLOT(1.3,1.4,-3)
      CALL SYMBOL(-.4,4.3,.16,CHAR(2),90.0,-1)
      CALL LINE(SI,E,MM,1,-1,2)
      CALL CURVE(SIA,EA,L,Z)
      CALL STAXIS(.1,.16,.1,.05,-1)
      CALL AXIS(0.,0.,'SPECIFIC IMPULSE',-16,8.,0.,0.,500.)
      CALL AXIS(0.,0.,'EFFICIENCY(%) = ',16,6.,90.,0.,10.)
      CALL PLOT(0.0,0.0,999)
      WRITE(*,986)
  986 FORMAT(1X,'ENTER 0 IF DONE, 1 IF NOT')
      READ(*,987) LLL
  987 FORMAT(I1)
      IF(LLL.EQ.0) GO TO 983
      GO TO 984
  983 CONTINUE
      STOP
      END
```

THIS DATA WAS OBTAINED FROM THE VARIABLE GEOMETRY MPD THRUSTER AT THE AIR FORCE ROCKET PROPULSION LABORATORY ON 13 JAN 86 AT 0807 HOURS. VOLTAGE (V) AND CURRENT (J) MEASUREMENTS WERE READ FROM AN OSCILLOSCOPE ATTACHED TO THE THRUSTER ELECTRODES. THE TOTAL IMPULSE (TI) WAS TAKEN FROM A TIME INTEGRATED ACCELEROMETER. TOTAL GAS PULSE IMPULSE (TIG) WAS OBTAINED FROM FIRING THE THRUSTER WITH THE ELECTRODES SHORTED. THE DURATION OF THE THRUST PULSE (DT) CAME FROM MEASURING THE TIME BETWEEN THE HALF CURRENT POINTS ON A PLOT OF CURRENT VS TIME. THE RISE AND FALL OF THE CURRENT WAS FAST ENOUGH TO JUSTIFY THE SQUARE PULSE SHAPE ASSUMPTION INHERENT IN THIS PROCEDURE. THE MASS FLOW RATE(DM) WAS DETERMINED BY MEARURING THE SHAPE OF THE GAS PULSE WITH AN ION GAUGE AND COMBINING THIS WITH THE MASS LOST FROM A PLENUM TO THE GAS VALVE.

CALCULATED DATA WAS OBTAINED FROM THE MEASURED DATA USING THE FOLLOWING EQUATIONS:

THRUST(T) = (TI-TIG)/DT

SPECIFIC IMPULSE = T/(9.8*DM)

EFFICIENCY = T**2/(2*V*J*DM)

AVERAGES OF REPEATED FIRINGS ARE SENT TO A PLOTTING PROGRAM WHICH FITS A SPLINED CURVE TO THEM. THRUSTER #27.410.0 .36.

CATHODE=27.4 CM	ANODE=10.0 CM	BENCHMARK SCALE= .3

GAS IMPULSE	THRUST PULSE DURATION	MASS FLOW RATE
.0010(N-S)	.0010(S)	.0060(KG/S)

VOLTAGE	AMPERES	TOTAL IMP.(N-S)	ISP	EFFICIENCY(%)
64.0	14900.	.031	510.	7.9
65.0	15000.	.032	527.	8.2
66.0	15100.	.033	544.	8.6
74.0	16900.	.041	680.	10.7
75.0	17000.	.042	697.	11.0
76.0	17100.	.043	714.	11.3
98.0	22800.	.068	1139.	16.7
100.0	23000.	.070	1173.	17.3
102.0	23200.	.072	1207.	17.8
145.0	33800.	.122	2058.	24.9
150.0	34000.	.124	2092.	24.7
155.0	34200.	.126	2126.	24.6
195.0	35800.	.168	2840.	33.3
200.0	36000.	.170	2874.	33.1
205.0	36200.	.172	2908.	32.8
250.0	38800.	.190	3214.	30.7
260.0	39000.	.194	3282.	30.6
270.0	39200.	.198	3350.	30.6

SPECIFIC IMPULSE *10^2 = ⊙
0 10 20 30 40 50 60
EFFICIENCY (%) = △
0 10 20 30 40 50 60
VOLTAGE (VOLTS) = □
0 60 120 180 240 300 360
CURRENT (KA)
0 6 12 18 24 30 36 42
THRUSTER #27.410.0 .36.

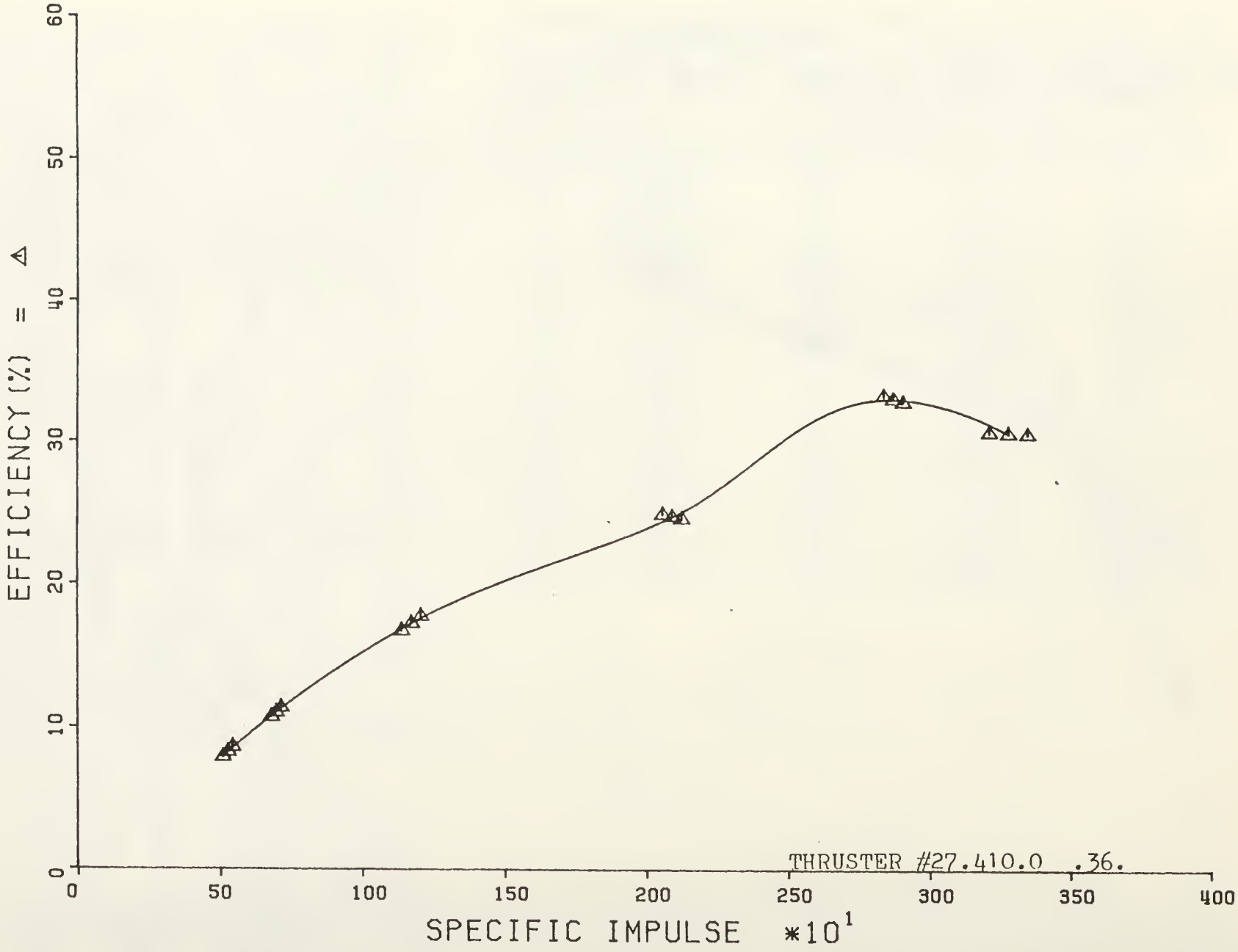
EFFICIENCY (%) = Δ
0
10
20
30
40
50
60
0
50
100
150
200
250
300
350
400
SPECIFIC IMPULSE *10¹
THRUSTER #27.410.0 .36.

APPENDIX B
THEORETICAL MODEL PROGRAM

```
      PROGRAM MPDI
      REAL J
      F(X)=1.00E-7*(J**4.0/X**2.0-4.94E-12*J**6.0*(X**2.0-2
     1.0*XMIN*X+XMIN**2.0))**0.5
      FF(X)=1.00E-7*(J**4.0/X**2.0-4.94E-12*J**6.0*(XMAX**2.
     10-2.0*XMAX*X+X**2.0))**0.5
  001 CONTINUE
      WRITE(*,010)
  010 FORMAT(1X,'THIS PROGRAM CALCULATES THE SUM OF THE'
     1,' BLOWING, PUMPING, AND ELECTROTHERMAL      THRUST '
     2,'COMPONENTS FOR AN MPD THRUSTER')
      WRITE(*,005)
  005 FORMAT(1X,'ENTER ANODE LENGTH IN F4.1 CM')
      READ(*,006) Z
  006 FORMAT(F5.2)
      WRITE(*,007)
  007 FORMAT(1X,'ENTER THE MASS FLOW RATE IN KG/S IN F7.5')
      READ(*,008) W
  008 FORMAT(F8.6)
      WRITE(*,020)
  020 FORMAT(1X,'ENTER THE CATHODE RADIUS IN F4.1 CM')
      READ(*,030) XMIN
  030 FORMAT(F5.2)
      WRITE(*,040)
  040 FORMAT(1X,'ENTER THE ANODE RADIUS IN F4.1 CM')
      READ(*,050) XMAX
  050 FORMAT(F5.2)
  056 FORMAT(F7.1)
      WRITE(*,060)
  060 FORMAT(1X,'ENTER AN EVEN NUMBER OF INTERVALS IN I100')
      READ(*,070) N
C     N=10
  061 CONTINUE
      WRITE(*,055)
  055 FORMAT(1X,'ENTER AMPERES IN F7.1')
      READ(*,056) J
  070 FORMAT(I100)
      H=(XMAX-XMIN)/(2.0*N)
      A=0.0
      AA=0.0
      AAA=0.0
      X=XMIN
      XXX=(XMAX+XMIN)/2.0
      DO 100 I=1,N
      XX=X+H
```

```
      XXXX=XXX+H
      A=A+H*(F(X)+F(XX))/2.0
      AA=AA+H*(FF(XXX)+FF(XXXX))/2.0
      X=XX
      XXX=XXXX
  100 CONTINUE
      AAA=A+AA
      WRITE(*,130) AAA
  130 FORMAT(1X,'BLOWING THRUST = ',F8.4)
      A=XMAX
      B=XMIN
      Y=(XMIN+XMAX)/2.0
      AAAA=4.44E-13*(7.0*Y**3.0/6.0-(B**3.0+A**3.0)/3.0-(A*B
     1**2.0+B*A**2.0)/4.0-(Y**2.0/2.0)*(A*LOG(Y/A)+B*LOG(Y/B
     2))+(A*B**2.0*LOG(B/A)+B*A**2.0*LOG(A/B))/2.0)*J**3.0/Z
      WRITE(*,131) AAAA
  131 FORMAT(1X,'PUMPING THRUST =',F8.4)
      AAAAA=3.25E-7*J**1.5*W**0.3*3.14159*(XMAX**2.0-XMIN**2
     1.0)
      WRITE(*,132) AAAAA
  132 FORMAT(1X,'ELECTROTHERMAL THRUST =',F8.4)
      AX=AAA+AAAA+AAAAA
      WRITE(*,133) AX
  133 FORMAT(1X,'TOTAL THRUST =',F8.4)
      A1=(55.4-26.31*(1-XMAX/5.1)-23.4*(1-Z/21.6))
      B1=(39.214-65.84*(1-XMAX/5.1)-27.656*(1-Z/21.6))*1E-4
      C1=(35.7-54.5*(1-XMAX/5.1)+3.88*(1-Z/21.6))*1E-8
      V=(A1-B1*J+C1*J**2)*(178.-47.3*1000.*W+4.3*(1000.*W)
     1**2)/49.
      WRITE(*,200) V,J
  200 FORMAT(1X,'VOLTAGE =',F9.4,2X,'CURRENT =',F7.1)
      YX=AX/(W*9.8)
      WRITE(*,134) YX
  134 FORMAT(1X,'SPECIFIC IMPULSE =',F8.3)
      E=(.5*W*(YX*9.8)**2.0)/(V*J)
      WRITE(*,201) E
  201 FORMAT(1X,'EFFICIENCY =',F8.4)
      P=V*J
      WRITE(*,222) P
  222 FORMAT(1X,'POWER =',F9.1)
      WRITE(*,140)
  140 FORMAT(1X,'ENTER 1 TO START OVER, 2 TO CHANGE CURREN'
     1'T ONLY')
      READ(*,150) M
  150 FORMAT(I1)
      IF(M.EQ.1) GO TO 001
      IF(M.EQ.2) GO TO 061
  151 CONTINUE
      STOP
      END
```

LIST OF REFERENCES

1. Jahn, R. G., Physics of Electric Propulsion, McGraw Hill Book Company Inc., New York, 1968.

2. Kuriki, K., and Shimizu, Y., MPD Arcjet System Performance Test, Report from the Institute of Space and Astronautical Science, Tokyo 153, Japan, 1983

3. Rudolpf, L. K., MPD Thruster Definition Study, Air Force Rocket Propulsion Laboratory, Edwards AFB CA, Contract Number AFRPL-TR-84-046, July 1984

4. Cory, J. S., Mass, Momentum, and Energy Flow From an MPD Thruster, Ph.D. Thesis, Princeton University, Princeton, N. J., September 1971

5. Rudolph, L. K., The MPD Thruster Onset Current Performance Limitation, Ph.D. Thesis, Princeton University, Princeton, N.J., November 1980.

6. King, D. Q., Jahn, R. G., and Clark, K. E.,Magnetoplasmadynamic Channel Flow for Design of Coaxial MPD Thrusters, Ph.D. Thesis, Princeton University, Princeton, N.J., Dec. 1981.

7. Harstad,K., Electrode Processes in MPD Thrusters, JPL Publication 81-114, California Institute of Technology, Pasadena, CA, March 1, 1982

8. Jahn, R. G., Pulsed Electromagnetic Gas Acceleration Report 634ac, Princeton University, Princeton, N. J., April 1978

9. Jahn, R. G., Pulsed Electromagnetic Gas Acceleration, Report 634ab, Princeton University, Princeton, N. J., January 1977

10. Mead, F. B. and Jahn, R. G., Scaling Characteristics of MPD Propulsion, paper presented at the 14th International Electric Propulsion Conference, Princeton, N. J., 30 Oct. - 1 Nov. 1979.

11. Kaplan, D. I. and Jahn, R. G., Performance Characteristics of Geometrically-Scaled Magnetoplasmadynamic (MPD) Thrusters, M.S.E. Thesis, Princeton University, Princeton, N.J., Feb. 1982.

12. Chen, F. F., Plasma Physics and Controlled Fusion, second ed., v. 1, Plenum Press, New York, 1984.

13. Martinache, G. H. C., A Theory on the Parallel-Plate Accelerator, Ph.D. Thesis, Princeton University, Princeton, N.J., May 1974

INITIAL DISTRIBUTION LIST

		No. Copies
1.	Defense Technical Information Center Cameraon Station Alexandria, Virginia 22304-6145	2
2.	Distinguished Professor (Emeritus) A. E. Fuhs Code 72, Space Systems Academic Group Naval Postgraduate School Monterey, California 93943-5000	1
3.	Library, Code 0142 Naval Postgraduate School Monterey, California 93943-5002	2
4.	Department Chairman, Code 67 Department of Aeronautics Naval Postgraduate School Monterey, California 93943	1
5.	Chairman, Space Systems Academic Group, Code 72 Naval Postgraduate School Monterey, California 93943	2
6.	Professor G. E. Latta, Code 54Lz Department of Mathematics Naval Postgraduate School Monterey, California 93943	1
7.	Professor R. E. Ball, Code 67Bp Department of Aeronautics Naval Postgraduate School Monterey, California 93943	1
8.	Professor D. W. Netzer, Code 67Nt Department of Aeronautics Naval Postgraduate School Monterey, California 93943	1
9.	Professor F. R. Schwirzke, Code 61Sw Department of Physics Naval Postgraduate School Monterey, California 93943	1
10.	Professor A. W. Cooper, Code 61Cr Department of Physics Naval Postgraduate School Monterey, California 93943	1

11. Wayne M. Schmidt, Captain, USAF 2
1148 East Ave J-5
Lancaster CA, 93535

Thesis
S33728 Schmidt
c.1 Effects of scaling on
the performance of
magnetoplasmadynamic
thrusters.